Power System Fundamental Frequency Estimation Using Unscented Kalman Filter

Cheng Qian, *Graduate Student Member, IEEE*, Mladen Kezunovic, *Life Fellow, IEEE*

Dept. of Electrical and Computer Engineering
Texas A&M University, College Station
College Station, TX, US
peterqiancheng@tamu.edu, kezunov@ece.tamu.edu

***Abstract*—Fundamental frequency is one of the most vital metrics of the power grid. Numerous frequency estimation techniques have been proposed, which are based on parameterization of deterministic signal models. Cautions should be taken since uncertainties such as noise are common in raw waveform measurements, and will propagate into estimation results. In order to mitigate the adverse impact of measurement noise, most recently, Kalman filter-based approaches were promoted, and are giving promising results. Nevertheless, conventional Kalman filter or extended Kalman filter have limited performance due to the high nonlinearity of the underlying state equations. In order to adapt to nonlinearity, this paper proposed a technique that leverages the Unscented Kalman Filter (UKF). The paper also introduces an approach that employs three-phase measurements to improve the overall frequency estimation accuracy. Simulation results show that the proposed UKF-based approach achieves extremely high fundamental frequency calculation accuracy despite severe noise interference.**

***Index Terms*—Frequency estimation, Kalman filter, uncertainty, unscented Kalman filter, power system measurement**

I. Introduction

Fundamental frequency is one of most crucial indicators to assess the operating conditions of the power grids, as it is directly determined by the spinning speed of synchronous generators. Numerous control applications rely on the accurate provision of fundamental frequency, such as underfrequency protective relays [1], power system stabilizers (PSS) [2], and islanding detection [3].

A number of frequency estimation methods have been designed, which employed a wide spectrum of signal processing/control techniques, including phase-locked-loops (PLLs) [4], Fourier transforms [5], and curve-fitting approaches [6]. The aforementioned frequency estimation algorithms utilize deterministic signal models, where uncertainties and noise terms are not represented, even though they are prevalent in raw power system waveform measurements. The uncertainties in waveform measurements will propagate through algorithms and reflect on the uncertainties in frequency estimation results.

Most recently, statistical tools are employed so that the impact of noise uncertainties can be effectively mitigated. Kalman filter is one of the most widely acclaimed techniques and has been leveraged in other areas of power system research, such as dynamic state estimation [7], harmonic parameter estimation [8], and frequency estimation [9]. Kalman filter was originally designed only for systems described by linear state equations. When the additive noise in waveform measurements is additive white Gaussian noise (AWGN), and system state equations are linear, Gaussianity is preserved through linear transforms. As a result, the propagation of AWGN in observations and states yields AWGN in further iterations, and Kalman filter is designed to be optimal in terms of achieving minimum mean squared error (MMSE) [10].

The frequency term in power waveforms, however, is embedded in highly nonlinear sine or cosine functions. When the system state equation is nonlinear, the noise components in observations and states are no long Gaussian. To apply Kalman filter to systems characterized by nonlinear state equations, extended Kalman filter (EKF) [9],[11] was created. The notion of EKF is based upon linearizing nonlinear system equations at the working point using Taylor approximation, where only the first two linear terms are preserved. The efficacy of EKF depends on the level of nonlinearity of system equations around the working point. As a result, EKF is only adequately accurate when the system equations are almost linear around the realistic range of working points. For power system, this range is between 55Hz to 65Hz. As is later shown in Section II, the waveform equations are highly nonlinear around such range, making EKF ineffective.

In order to complement the performance of EKF under highly nonlinear conditions, unscented Kalman filter (UKF) was proposed in 1997 [12], and later elaborated in [13]. UKF is based on unscented transform (UT), where the statistical characteristics of the distribution after nonlinear transform are estimated with higher accuracy than letting statistics propagate through linearized system equations, as is practiced in EKF. Paper [14] introduced a UKF-based technique for fundamental frequency estimation using the instantaneous real and reactive

This work was supported by the DoE/NETL "Timing Intrusion Management Ensuring Resiliency" (TIMER) project funded under the CEDS program.

power equations. The assumption is that both voltage and current waveform measurements conform to a sinusoidal form. In reality, however, current waveforms may be highly distorted, making the aforementioned technique highly unreliable.

This paper proposes an alternative approach to estimating fundamental frequency using UKF, where only the waveform measurements are used. Simulation results show that the proposed approach can achieve extremely high frequency estimation accuracy even in the case of low signal-to-noise ratio (SNR). The rest of the paper is organized as follows: Section II discusses the system equations used in UKF; Section III introduces the frequency estimation algorithm based on UKF; simulations are conducted in Section IV, and the results are analyzed; Conclusions are outline at the end.

II. Instantaneous Waveform Models

Either single-phase or three-phase voltage waveform measurements can be used in the proposed approach. Signal models in both cases are designed.

A. Single-Phase Waveform Model

The sinusoidal voltage waveforms can be denoted by:

$$x_k = A \cdot \cos(\omega k \Delta t + \phi_0) \tag{1}$$

where A is amplitude, ω is angular frequency, k is sample index, Δt is sampling interval, and ϕ_0 is initial phase angle.

Therefore, consecutive samples at time steps $(k+1)$ and $(k+2)$ can be expressed as:

$$x_{k+1} = A \cdot \cos[\omega(k+1)\Delta t + \phi_0] \tag{2a}$$

$$x_{k+2} = A \cdot \cos[\omega(k+2)\Delta t + \phi_0] \tag{2b}$$

It can be proven that:

$$x_{k+2} + x_k = 2x_{k+1} \cdot \cos(\omega \Delta t) \tag{3}$$

Equation (3) is the fundamental state update equation employed in paper [9].

B. Three-Phase Waveform Model

Electric power is transmitted through three-phase transmission system, with 120° electric phase angle displacement between any two phases. This phase angle displacement is determined by the symmetric design of synchronous generators, and thus always holds true.

Denote phase A voltage as x_k, phase B voltage as y_k, and phase C voltage as z_k. Then,

$$y_k = A \cdot \cos\left(\omega k \Delta t + \phi_0 - \frac{2}{3}\pi\right) \tag{4a}$$

$$z_k = A \cdot \cos\left(\omega k \Delta t + \phi_0 + \frac{2}{3}\pi\right) \tag{4b}$$

It can be shown that y_k can be conveniently expressed with phase A waveform measurements, shown in (5):

$$\begin{aligned} y_k = {} & A \cdot \cos(\omega k \Delta t + \phi_0)\cos\left(-\frac{2}{3}\pi\right) \\ & -A \cdot \sin(\omega k \Delta t + \phi_0)\sin(-\frac{2}{3}\pi) \end{aligned} \tag{5}$$

$$= x_k \cos\left(-\frac{2}{3}\pi\right) + \frac{x_k \cos(\omega\Delta t) - x_{k-1}}{\sin(\omega \Delta t)} \sin\left(-\frac{2}{3}\pi\right)$$

Similarly,

$$z_k = x_k \cos\left(\frac{2}{3}\pi\right) + \frac{x_k \cos(\omega\Delta t) - x_{k-1}}{\sin(\omega \Delta t)} \sin\left(\frac{2}{3}\pi\right) \tag{6}$$

Besides, similar to (3), for both phase B and phase C waveform samples:

$$y_{k+2} + y_k = 2y_{k+1} \cdot \cos(\omega \Delta t) \tag{7a}$$

$$z_{k+2} + z_k = 2z_{k+1} \cdot \cos(\omega \Delta t) \tag{7b}$$

III. Fundamental Frequency Estimation Using UKF

In order to apply UKF in frequency estimation, waveform equations should be expressed as state equations, in which frequency parameter is embedded. The selection of sigma points is also discussed in this section.

A. Shortcomings of EKF Model and Approach

From (3), frequency can be mathematically derived by taking the inverse of cosine function:

$$f = \frac{1}{2\pi\Delta t} \cdot \cos^{-1}\left(\frac{x_{k+2} + x_k}{2x_{k+1}}\right) \tag{8}$$

where f is the instantaneous fundamental frequency in Hertz.

When the sampling frequency of a field device is adequately high, the argument in the inverse cosine function is close to 1. Consequently, the working point of the nonlinear equation is at the most nonlinear part of the inverse cosine function. As a result, the EKF-based method introduced in [9] will incur large error.

As previous discussed, UT can be used in this case to yield more realistic estimates in terms of the propagation of statistics (first two moments, in particular) of input variables through nonlinear transform [12]-[13].

B. State-Space Representation

In order to use Kalman filter-type techniques, the problem has to be represented in the form of state-space models. Choosing the states and measurement variables as follows:

$$\begin{gathered} x_{1,k} = x_k, x_{2,k} = x_{k-1}, x_{3,k} = \omega\Delta t \\ y_{1,k} = x_k, y_{2,k} = y_k, y_{3,k} = z_k \end{gathered} \tag{9}$$

As a result, the state update equation and measurement input equation can be expressed as:

$$x_{1,k+1} = -x_{2,k} + 2x_{1,k}\cos(x_{3,k}) \tag{10a}$$

$$x_{2,k+1} = x_k = x_{1,k} \tag{10b}$$

$$x_{3,k+1} = x_{3,k} \tag{10c}$$

$$y_{1,k+1} = x_{1,k+1} \tag{10d}$$

$$
\begin{aligned}
&y_{2,k+1} \\
&= x_{1,k+1}\cos\left(\frac{2}{3}\pi\right) \\
&- \frac{x_{1,k+1}\cos\left(x_{3,k+1}\right) - x_{2,k+1}}{\sin(x_{3,k+1})}\sin\left(\frac{2}{3}\pi\right)
\end{aligned} \tag{10e}
$$

$$
\begin{aligned}
&y_{3,k+1} \\
&= x_{1,k+1}\cos\left(\frac{2}{3}\pi\right) \\
&+ \frac{x_{1,k+1}\cos\left(x_{3,k+1}\right) - x_{2,k+1}}{\sin(x_{3,k+1})}\sin\left(\frac{2}{3}\pi\right)
\end{aligned} \tag{10f}
$$

Note that $x_{3,k} = \omega\Delta t = 2\pi f\Delta t$, where Δt is the sampling interval. Therefore, frequency is estimated through:

$$f = \frac{x_{3,k}}{2\pi\Delta t} \tag{11}$$

When only single-phase measurements are available, (10a)-(10d) should be used; when additional observations of the other two phases are present, (10e) and (10f) can be incorporated.

C. *Selection of Sigma Points and Their Propagation in State Equations*

In UKF, sigma points are a collection of samples from the original distribution, deterministically chosen in such a way that the first two moments of sigma points preserve the first two moments of the original distributions. The sigma points are then propagated to the new distribution through the nonlinear function, where the statistics of the new distribution can be calculated using the propagated sigma points. The selection of sigma points are done in the following way [12]-[14]:

$$
\begin{gathered}
\chi_0 = \bar{x} \\
\chi_i = \bar{x} + \left(\sqrt{(n+\lambda)P_{xx}}\right)_i, i = 1,2,\dots,n \\
\chi_{i+n} = \bar{x} - \left(\sqrt{(n+\lambda)P_{xx}}\right)_i
\end{gathered} \tag{12}
$$

where n is the number of states, $\lambda = \alpha^2(n+\kappa)$, $\left(\sqrt{(n+\lambda)P_{xx}}\right)_i$ is the *i*th column of the square root of matrix $(n+\lambda)P_{xx}$, and can be efficiently calculated using by Cholesky decomposition.

The sigma points are then propagated through the nonlinear function $\gamma_i = f(\chi_i)$, where the first two moments of the new distribution can be calculated as follows:

$$\bar{y} = \sum_{i=0}^{2n} W_i^{(m)}\gamma_i \tag{13a}$$

$$P_{yy} = \sum_{i=0}^{2n} W_i^{(c)}[(\gamma_i - \bar{y})(\gamma_i - \bar{y})^T] \tag{13b}$$

where weights $W_i^{(m)}$ and $W_i^{(c)}$ are defined as follows:

$$W_0^{(m)} = \frac{\lambda}{n+\lambda}, W_0^{(c)} = W_0^{(m)} + (1 - \alpha^2 + \beta) \tag{14a}$$

$$W_i^{(m)} = W_i^{(c)} = \frac{1}{2(n+\lambda)}, i = 1,2,\dots,n \tag{14b}$$

In (12)-(14), factors $\alpha$and κ are used to provide fine-tuning of the "spread" of sigma points around the mean $\chi_0 = \bar{x}$. Parameter β is used to incorporate information about higher moments of the original distribution. There is no uniform method to select sigma points, and the available approaches are described in detail in [15].

IV. IMPLEMENTATION AND SIMULATIONS

The proposed technique is implemented in MathWorks Simulink software. Sampling frequency is 6kHz. In order to evaluate the states defined in (10) at each time step, both EKF and UKF are used. Three sets of simulations are conducted to demonstrate better performance of UKF-based approach over EFK-based approach in the formulated frequency estimation problem: EKF using three-phase measurements, UKF using three-phase measurements, UKF using single-phase measurement. The performance of the three strategies are evaluated through metrics including optimality/bias, and sensitivity toward initial values.

A. *Test Scenarios and Evaluation Metrics*

To test the performance of the proposed approach in various power system operating conditions, both steady-state and dynamic-state waveforms are used in the simulation, including pure sinusoidal signals, steady-state signals with harmonic infiltration, amplitude-modulated signals, phase-modulated signals, and frequency ramping signals. Test signal parameters are determined based on IEEE standard [16]. AWGN is added to pure sinusoidal signals, where the SNR is either 20dB or 40dB. The SNR is defined as:

$$\mathrm{SNR} = 10\cdot\log_{10}\left(\frac{\sigma^2_{\mathrm{signal}}}{\sigma^2_{\mathrm{noise}}}\right) = 20\cdot\log_{10}\left(\frac{A_{\mathrm{signal}}}{A_{\mathrm{noise}}}\right) \tag{15}$$

where σ^2 is the variance, A is the root-mean-square (RMS) amplitude. Practically, A_{noise} is the standard deviation of noise, i.e. σ_{noise}.

As discussed before, since the system equation is highly nonlinear, neither EKF nor UKF will attain optimality, in terms of achieving MMSE solutions. This sub-optimality condition will result in bias between estimated fundamental frequency and "true" theoretical frequency. Besides, the initial conditions consist of current step sample, previous step sample, and angular increment over one sampling interval (proportional to angular frequency). Depending on the initial conditions for states, the nonlinearity of state equations may lead to undesired though mathematically valid solutions, if not causing divergence. Thus, the sensitivity to initial conditions should also be evaluated.

B. *Simulations with 40dB AWGN Input*

In this test scenario, 40dB SNR is associated with the signal uncertainty characterized by a standard deviation of 1% of the signal amplitude. The test signal is shown in Fig. 1(a) and (b).

- Frequency estimation bias:

Test results are shown in Table I. It can be observed that highly accurate frequency estimation results can be achieved by using either single-phase or three-phase waveform measurements.

TABLE I. SUMMARY OF FREQUENCY ESTIMATION BIAS

Case Details	*UKF-Single Phase*	*UKF-Three Phase*
Steady-state unbalanced	$< 5\times10^{-7}$ Hz	$< 5\times10^{-7}$ Hz
Steady-state harmonics	$< 5\times10^{-7}$ Hz	$< 5\times10^{-7}$ Hz
Amplitude modulation	$< 5\times10^{-7}$ Hz	$< 5\times10^{-7}$ Hz
Phase modulation	$< 5\times10^{-7}$ Hz	$< 5\times10^{-7}$ Hz
Frequency ramping	$< 5\times10^{-7}$ Hz	$< 5\times10^{-7}$ Hz

- Sensitivity to initial conditions:

As aforementioned, state x_3 is proportional to angular frequency $\omega = 2\pi f$, and its initial value is set to be nominal. States x_1 and x_2 are related to instantaneous sample values, and cannot be predicted, and thus are set arbitrarily to 1p.u. In the test, the selected initial values may deviated from the "true" starting point of the system states in either frequency or amplitude. Fundamental frequency of input test signal ranges from 55Hz to 65Hz, with 1Hz increment. Besides, the amplitude deviation between selected initial conditions and "true" amplitude may be anywhere between -100% and 100%. EKF approach is tested as well to show the comparison.

TABLE II. SUMMARY OF SENSITIVITY TO INITIAL CONDITIONS

Case Details	EKF-Three Phase	UKF-Three Phase
Frequency deviation ±1Hz to ±5Hz	Converge	Converge
Amplitude deviation ±50%	Diverge	Converge
Amplitude deviation ±25%	Diverge	Converge
Amplitude deviation ±10%	Converge	Converge

As can be observed, EKF-based approach may diverge when the selected initial values deviate more than 25% off the true values. In practice, this essentially means that the convergence depends on when the waveform samples are taken. There is at least 75% chance that EKF-based method may diverge. On the other hand, proposed UKF-based method will always converge.

C. Simulations with 20dB AWGN Input

In this test case, 20dB SNR is associated with the signal uncertainty characterized by a standard deviation of 10% of the signal amplitude. As can be seen in Fig. 1(c), the noise causes visibly significant distortion.

- Frequency estimation bias:

Test results are tabulated in Table III. Compared to the 40dB noise input case, higher noise level increases frequency estimation bias by at least 10 times. Three-phase measurements improve estimation accuracy than single-phase measurements. Regardless, the estimation accuracy is still sufficiently high.

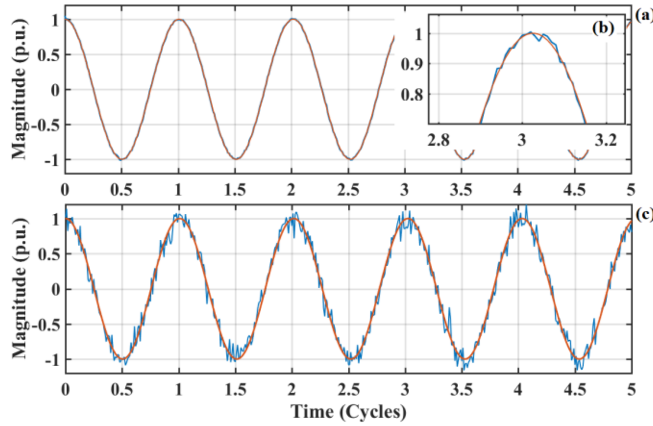

Figure 1. Test Waveforms: 59.5Hz Pure Cosine Wave with Noise Infiltration. (a). Sinusoidal wave with 40dB AWGN. (b). Local Zoom-in of the Waveform in (a). (c). Sinusoidal wave with 20dB AWGN. Orange curves are noiseless signals.

TABLE III. SUMMARY OF FREQUENCY ESTIMATION BIAS

Case Details	*UKF-Single Phase*	*UKF-Three Phase*
Steady-state unbalanced	$< 1\times10^{-5}$ Hz	$< 5\times10^{-6}$ Hz
Steady-state harmonics	$< 1\times10^{-6}$ Hz	$< 1\times10^{-6}$ Hz
Amplitude modulation	$< 5\times10^{-6}$ Hz	$< 2\times10^{-6}$ Hz
Phase modulation	$< 1\times10^{-6}$ Hz	$< 1\times10^{-6}$ Hz
Frequency ramping	$< 1\times10^{-6}$ Hz	$< 1\times10^{-6}$ Hz

- Sensitivity to initial conditions:

As shown in Table IV, similar to the 40dB noise input case, EKF-based approach is sensitive to the initial values of states x_1 and x_2. Consequently, there is at least 75% chance that EKF-based method does not converge.

TABLE IV. SUMMARY OF SENSITIVITY TO INITIAL CONDITIONS

Case Details	EKF-Three Phase	UKF-Three Phase
Frequency deviation ±1Hz to ±5Hz	Converge	Converge
Amplitude deviation ±50%	Diverge	Converge
Amplitude deviation ±25%	Diverge	Converge
Amplitude deviation ±10%	Converge	Converge

D. Influence of Sigma Point Selection on Estimation Bias

Due to the nonlinearity of state equations, the frequency estimation based on UKF will inevitably result in sub-optimal solutions, i.e. estimation biases. The tuning of UKF procedure, namely, the selection of parameters α, β, and κ in (12)-(14) will affect frequency estimation results. This is summarized in Table V. UKF-three phase test is used in this simulation, where this nominal frequency is 60.5Hz. The value shown in the table is the maximum estimation bias in all types of tests.

TABLE V. INFLUENCE OF SIGMA POINT SELECTION ON BIASES IN FREQUENCY ESTIMATION

Case Details	***20dB Noise***	***40dB Noise***
$\alpha = 1 \times 10^{-3}$ $\beta = 2, \kappa = 0$	5×10^{-4} Hz	5×10^{-4} Hz
$\alpha = 0.1$ $\beta = 2, \kappa = 0$	$< 5\times10^{-7}$ Hz	$< 5\times10^{-7}$ Hz
$\alpha = 0.1$ $\beta = 4, \kappa = 0$	1.5×10^{-6} Hz	5×10^{-7} Hz
$\alpha = 0.1$ $\beta = 2, \kappa = 2$	5×10^{-7} Hz	5×10^{-7} Hz

It can be concluded that sigma points should be carefully selected to achieve lowest estimation uncertainties. Even though $\alpha = 1 \times 10^{-3}$ is recommended in papers [12]-[14], it can be seen that this choice does not provide best estimation result in the context of power system frequency estimation. In practice, measurement noise may not necessarily be Gaussian. As a result, β parameter should be tuned accordingly.

V. CONCLUSIONS

The paper proposes a UKF-based fundamental frequency calculation approach using single or three-phase waveform measurements. Simulations demonstrate the comparison of proposed method with EKF-based method in terms of estimation bias, and sensitivity to initial conditions. The contributions are outlines as follows.

- The characteristics of noise propagating through the nonlinear system equations are estimated more accurately with UT, which resulted in better mitigation of noise impact on fundamental frequency calculation with the application of UKF.
- Despite the choice of initial conditions and the extreme nonlinearity of system equations, the proposed UKF-based method always converge to a solution. This is not observed in prior EKF-based method.
- Sub-optimality is achieved by choosing appropriate sigma points in the proposed method, where frequency calculation error can be reduced to minimal level.
- Simulations show that both single-phase and three-phase measurement based implementation will achieve sufficient frequency estimation accuracy, even when the noise level is as high as 10% of signal amplitude.

REFERENCES

[1]. Load Shedding, Load Restoration and Generator Protection Using Solid-state and Electromechanical Underfrequency Relays. [Online]. Available: https://store.gegridsolutions.com/faq/documents/489/GET-6449.pdf.

[2]. WECC Power System Stabilizer Tuning Guidelines. [Online]. Available: https://www.wecc.biz/Reliability/Power%20System%20Stabilizer%20Tuning%20Guidelines.pdf.

[3]. O. Samuelsson and N. Strath, "Islanding detection and connection requirements," 2007 IEEE Power Engineering Society General Meeting, Tampa, FL, 2007, pp. 1-6.

[4]. M. Karimi-Ghartemani, H. Karimi and M. R. Iravani, "A magnitude/phase-locked loop system based on estimation of frequency and in-phase/quadrature-phase amplitudes," in *IEEE Transactions on Industrial Electronics*, vol. 51, no. 2, pp. 511-517, April 2004.

[5]. J. Borkowski, D. Kania and J. Mroczka, "Interpolated-DFT-Based Fast and Accurate Fre-quency Estimation for the Control of Power," in *IEEE Transactions on Industrial Electronics*, vol. 61, no. 12, pp. 7026-7034, Dec. 2014.

[6]. A. K. Pradhan, A. Routray and A. Basak, "Power system frequency estimation using least mean square technique," in *IEEE Transactions on Power Delivery*, vol. 20, no. 3, pp. 1812-1816, July 2005.

[7]. E. Ghahremani and I. Kamwa, "Dynamic State Estimation in Power System by Applying the Extended Kalman Filter With Unknown Inputs to Phasor Measurements," in *IEEE Transactions on Power Systems*, vol. 26, no. 4, pp. 2556-2566, Nov. 2011.

[8]. S. Kumar Singh, N. Sinha, A. Kumar Goswami, and N. Sinha, "Several variants of Kalman Filter algorithm for power system harmonic estimation," in *International Journal of Electrical Power & Energy Systems*, vol. 78, pp. 793-800, June 2016.

[9]. A. Routray, A. K. Pradhan and K. P. Rao, "A novel Kalman filter for frequency estimation of distorted signals in power systems," in *IEEE Transactions on Instrumentation and Measurement*, vol. 51, no. 3, pp. 469-479, June 2002.

[10]. S.M. Kay. *Fundamentals of Statistical Signal Processing, Volumn I – Estimation Theory*. New Jersey: Prentice Hall, 1993.

[11]. A. Germani, C. Manes and P. Palumbo, "Polynomial extended Kalman filter," in *IEEE Transactions on Automatic Control*, vol. 50, no. 12, pp. 2059-2064, Dec. 2005.

[12]. S.J. Julier, J.K. Uhlmann, "A Consistent, Debiased Method for Converting Between Polar and Cartesian Coordinate Systems". [Online]. Available:https://pdfs.semanticscholar.org/b347/0d801eb1bd16d4e835a0d930613ee80ac29e.pdf. July 1997.

[13]. S. J. Julier and J. K. Uhlmann, "Unscented filtering and nonlinear estimation," in *Proceedings of the IEEE*, vol. 92, no. 3, pp. 401-422, March 2004.

[14]. P. Regulski and V. Terzija, "Estimation of Frequency and Fundamental Power Components Using an Unscented Kalman Filter," in *IEEE Transactions on Instrumentation and Measurement*, vol. 61, no. 4, pp. 952-962, April 2012.

[15]. H. M. T. Menegaz, J. Y. Ishihara, G. A. Borges and A. N. Vargas, "A Systematization of the Unscented Kalman Filter Theory," in *IEEE Transactions on Automatic Control*, vol. 60, no. 10, pp. 2583-2598, Oct. 2015.

[16]. IEEE Standard for Synchrophasor Measurements for Power Systems -- Amendment 1: Modification of Selected Performance Requirements," in *IEEE Std C37.118.1a-2014 (Amendment to IEEE Std C37.118.1-2011)*, vol., no., pp.1-25, Apr. 2014.